Supporting Information for

Hydrolytically stable nanosheets of Cu-Imidazolate MOF for selective trapping and simultaneous removal of multiple heavy metal ions.

Prathmesh Bhadane[a], Priya Mahato[a], Dhruv Menon[b], Biraj Kanta Satpathy[a], Lisi Wu[c], Swaroop Chakraborty[c], Prateek Goyal[a], Iseult Lynch[c], Superb K. Misra[a,*]

[a]*Materials Engineering, Indian Institute of Technology Gandhinagar, Gujarat 382355, India.*
[b]*Department of Chemical Engineering and Biotechnology, University of Cambridge, Cambridge, CB3 0AS, United Kingdom.*
[c]*School of Geography, Earth and Environmental Sciences, University of Birmingham, Edgbaston, Birmingham, B152TT, United Kingdom.*

***Email:** smisra@iitgn.ac.in

Equations:

Batch adsorption experiments

- $$Removal\ Efficiency\ (RE)(\%) = \frac{C_0 - C_e}{C_0} * 100$$ Eq. 1
- $$Adsorption\ capacity\ (q_e) = \frac{C_0 - C_e}{m} V$$ Eq. 2
- $$Distribution\ Coefficient\ (K_d) = \frac{C_0 - C_e}{C_e} \times \frac{V}{m}$$ Eq. 3

Where, C_0 and C_e (mg/L) represents initial and equilibrium concentration of Pb(II) in supernatant respectively. m (g) is adsorbent mass, V (ml) is solution volume.

Kinetics studies

- Pseudo first-order kinetics: $\ln(q_e - q_t) = \ln q_e - k_1 t$ Eq. 4
- Pseudo second-order kinetics: $\frac{t}{q_t} = \frac{1}{k_2 q_e^2} + \frac{t}{q_e}$ Eq. 5

Where, q_e and q_t represents the adsorption capacity at equilibrium and time t (mg/g), respectively. k_1 (min^{-1}) and k_2 (g $mmol^{-1}$ min^{-1}) represents parameters for kinetic rate constants for pseudo-first-order and pseudo-second-order model, respectively.

Adsorption isotherm studies

- Langmuir adsorption isotherm: $\frac{C_e}{q_e} = \frac{C_e}{q_{max}} + \frac{1}{k_1 q_{max}}$ Eq. 6
- Freundlich adsorption isotherm: $log\ q_e = log\ K_f + \frac{1}{n} log\ C_e$ Eq. 7
- $$Separation\ factor\ (R_L) = \frac{1}{1 + K_L C_o}$$ Eq. 8

Where, q_{max} and q_e represents the maximum (theoretical) and equilibrium adsorption capacity (mg/g) respectively, C_e is adsorbate concentration at equilibrium (mg/L), k_L (L/mg) and K_F (L/mg) represents *the Langmuir (represents the binding strength) and Freundlich constant (represent the adsorption capacity) respectively and 1/n (ranging 0-1) represent the adsorption intensity.*

<u>Adsorption</u> <u>thermodynamics</u> <u>studies</u>

- $$ln(K) = -\left(\frac{\Delta H^0}{R}\right)\frac{1}{T} + \frac{\Delta S^0}{R}$$ Eq. 9
- $$\Delta G^0 = \Delta H^0 - T\Delta S^0$$ Eq. 10

Where, K (q_e/C_e) represents the equilibrium constant (L/g), T representants temperature (K) and R (8.314 J mol^{-1} K^{-1}) represents gas constant.

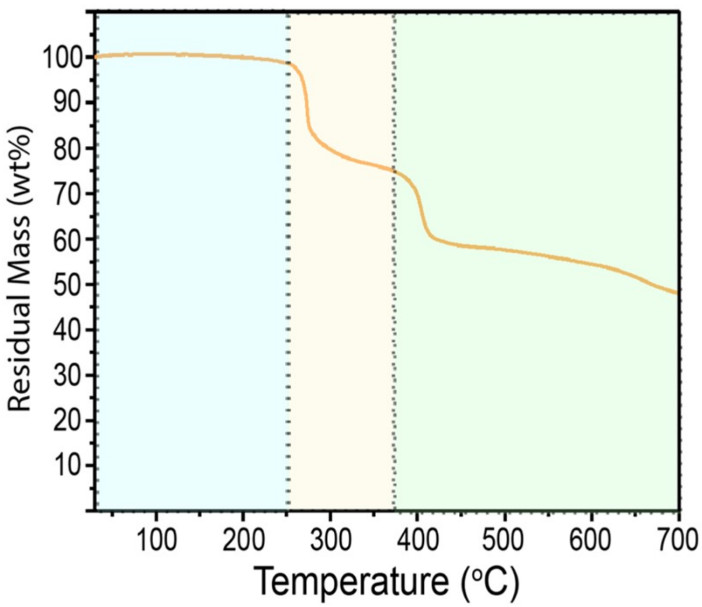

Fig. S1. Thermogravimetric analysis (TGA) of Cu-Im showing three distinctive regions of behaviour suggesting high thermal stability up to 240^{O}C.

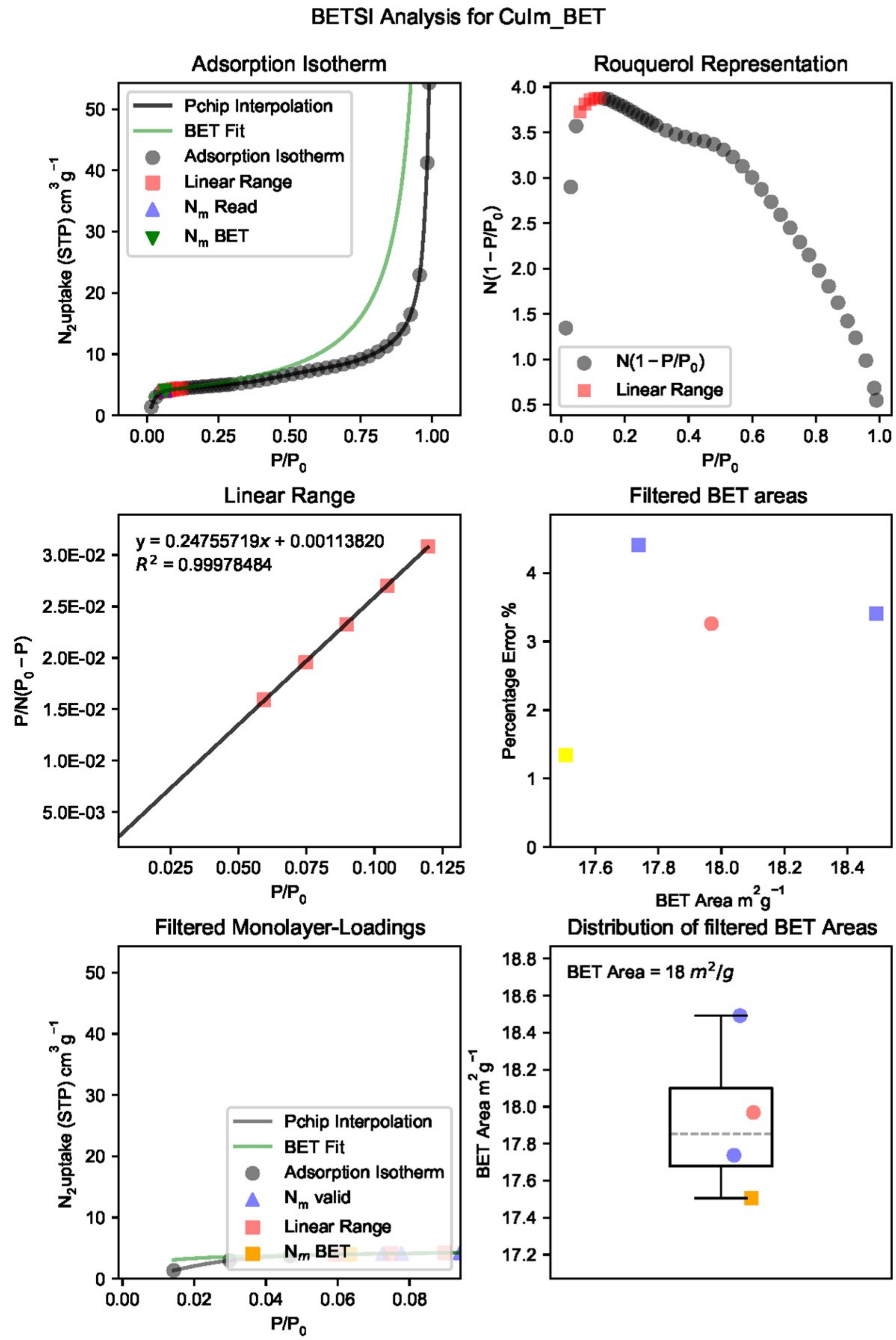

Fig. S2. Elaboration of the BET surface area using the Rouquerol criteria as implemented using the BETSI algorithm. BETSI predicts the BET surface area to be 18 m^2g^{-1}. For a detailed understanding of the implementation of this analysis, readers are directed to Fairen-Jimenez et al.[1]

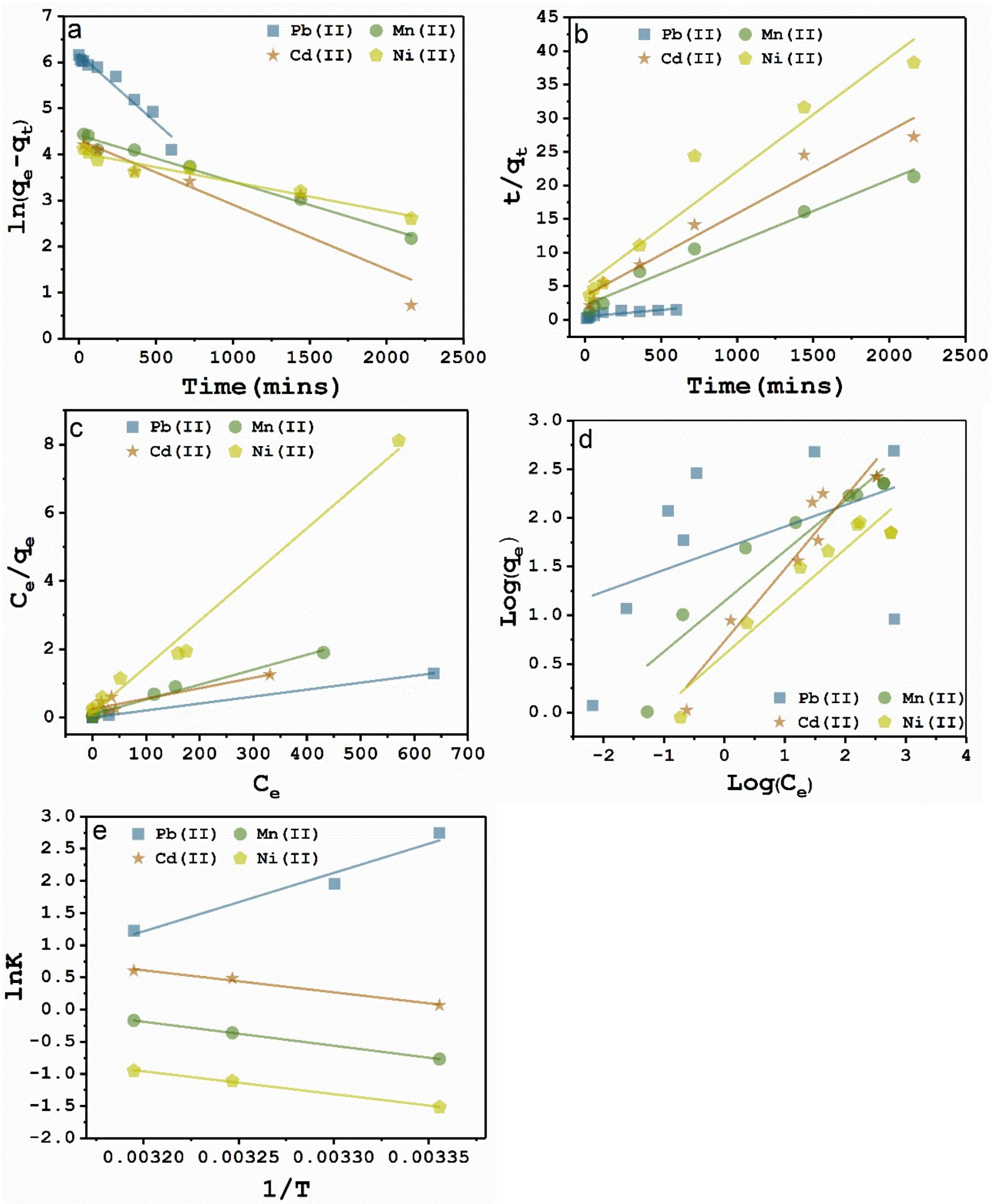

Fig S3. a. pseudo-first-order kinetics reaction linear fitted data, b. pseudo-second-order kinetics reaction linear fitted data, c. Langmuir adsorption isotherm, d. Freundlich adsorption isotherm, e. adsorption thermodynamics (Van't Hoff plot).

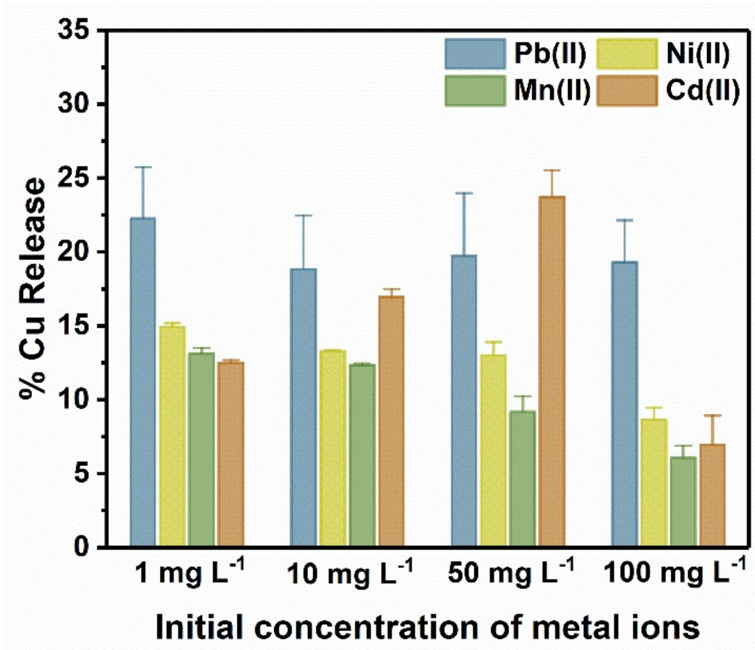

Fig. S4. Copper release profile. % Cu release profile for removal of heavy metal ions with varied initial metal concentration in ultrapure water. (MOF concentration: 1000 mg L^{-1}).

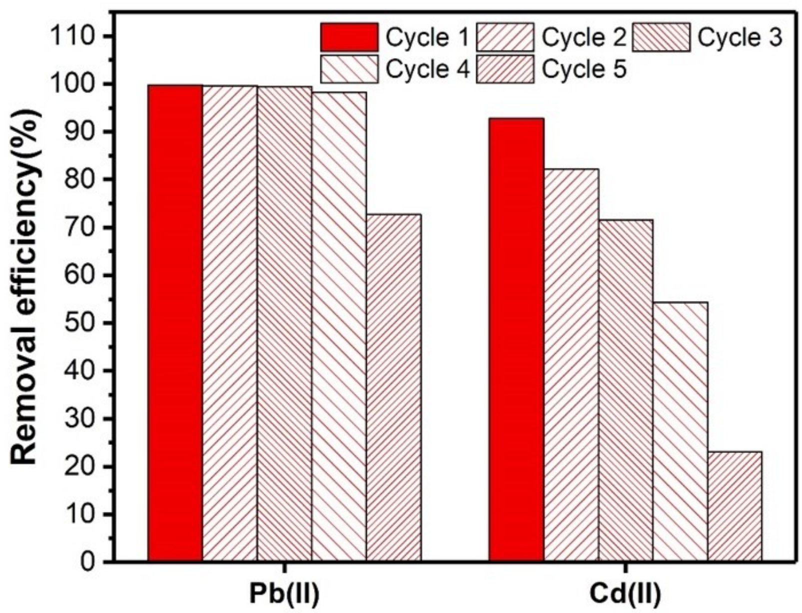

Fig. S5. Removal efficiency of Cu-Im MOF for metal ions adsorption over 5 cycles. (MOF concentration: 1000 mg L^{-1}, Initial metal ion concentration: 1 – 500 mg L^{-1} for Cd(II) and 1-1000 mg L^{-1} for Pb(II), at pH 5 and temperature: 25 ^{o}C).

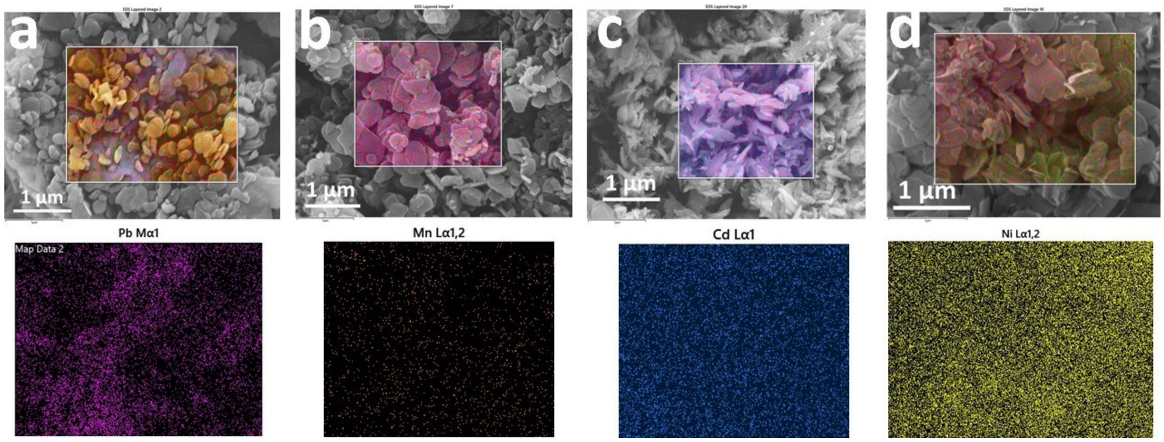

Fig. S6. Post-adsorption study using EDS elemental mapping, a. Pb adsorbed Cu-Im, b. Mn adsorbed Cu-Im, c. Cd adsorbed Cu-Im and d. Ni adsorbed Cu-Im.

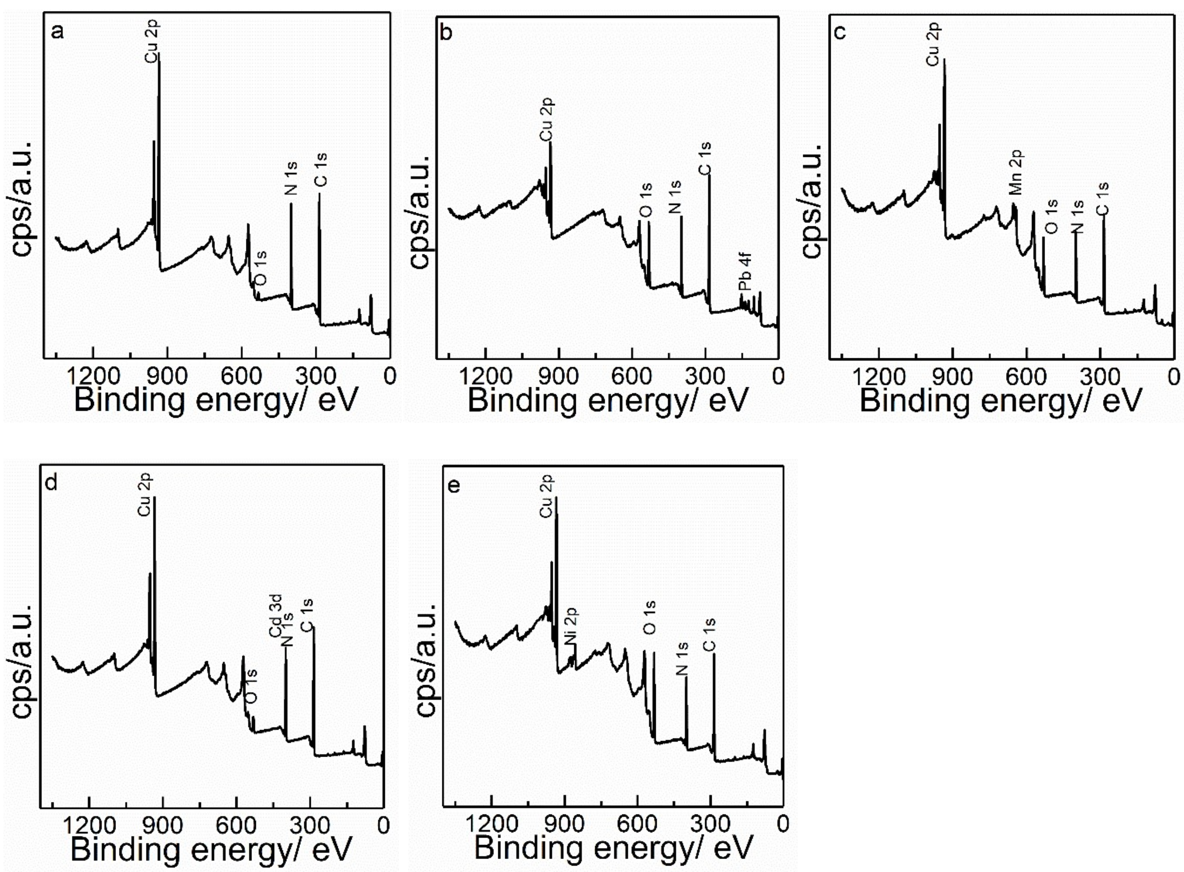

Fig. S7. XPS survey spectrum of a. pristine Cu-Im MOF, b. Pb adsorbed Cu-Im, c. Mn adsorbed Cu-Im, d. Cd adsorbed Cu-Im and e. Ni adsorbed Cu-Im.

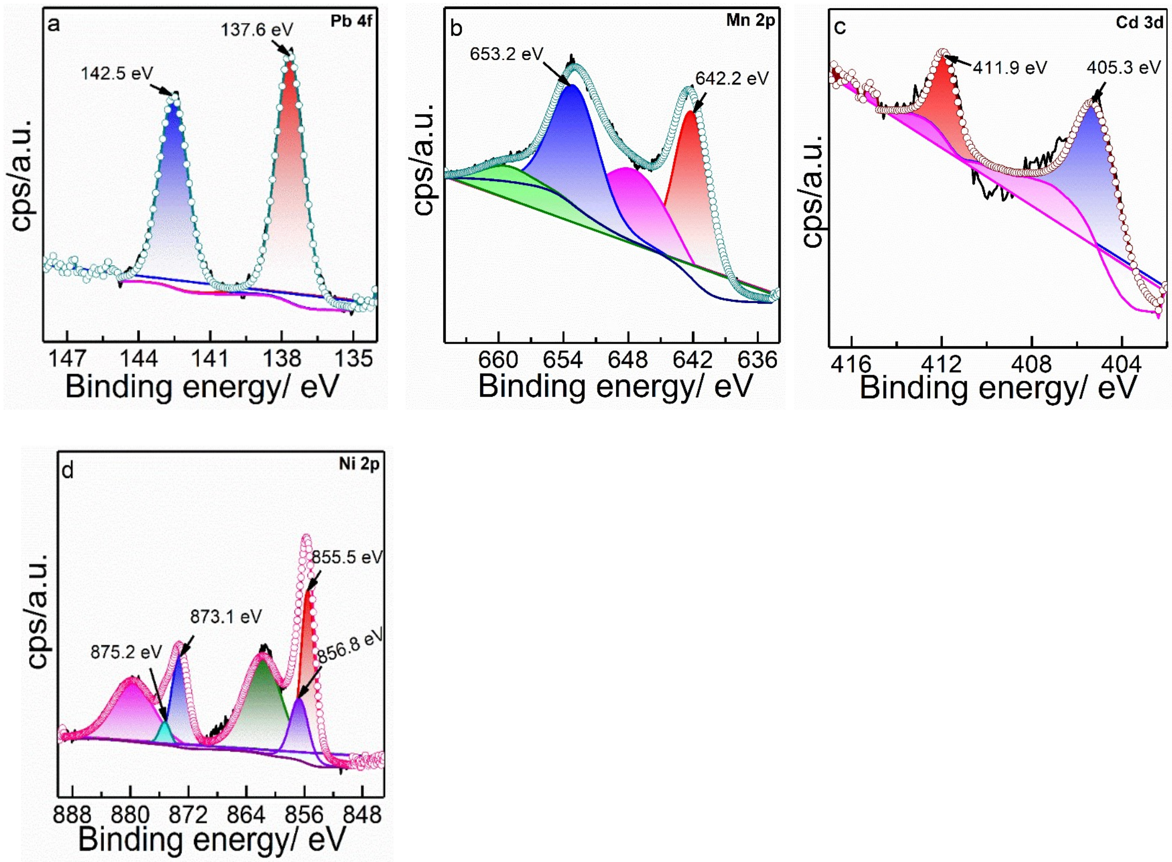

Fig. S8. XPS high resolution spectra of a. Pb 4f (in Pb adsorbed Cu-Im), b. Mn 2p (in Mn adsorbed Cu-Im), c. Cd 3d (in Cd adsorbed Cu-Im), d. Ni 2p (in Ni adsorbed Cu-Im).

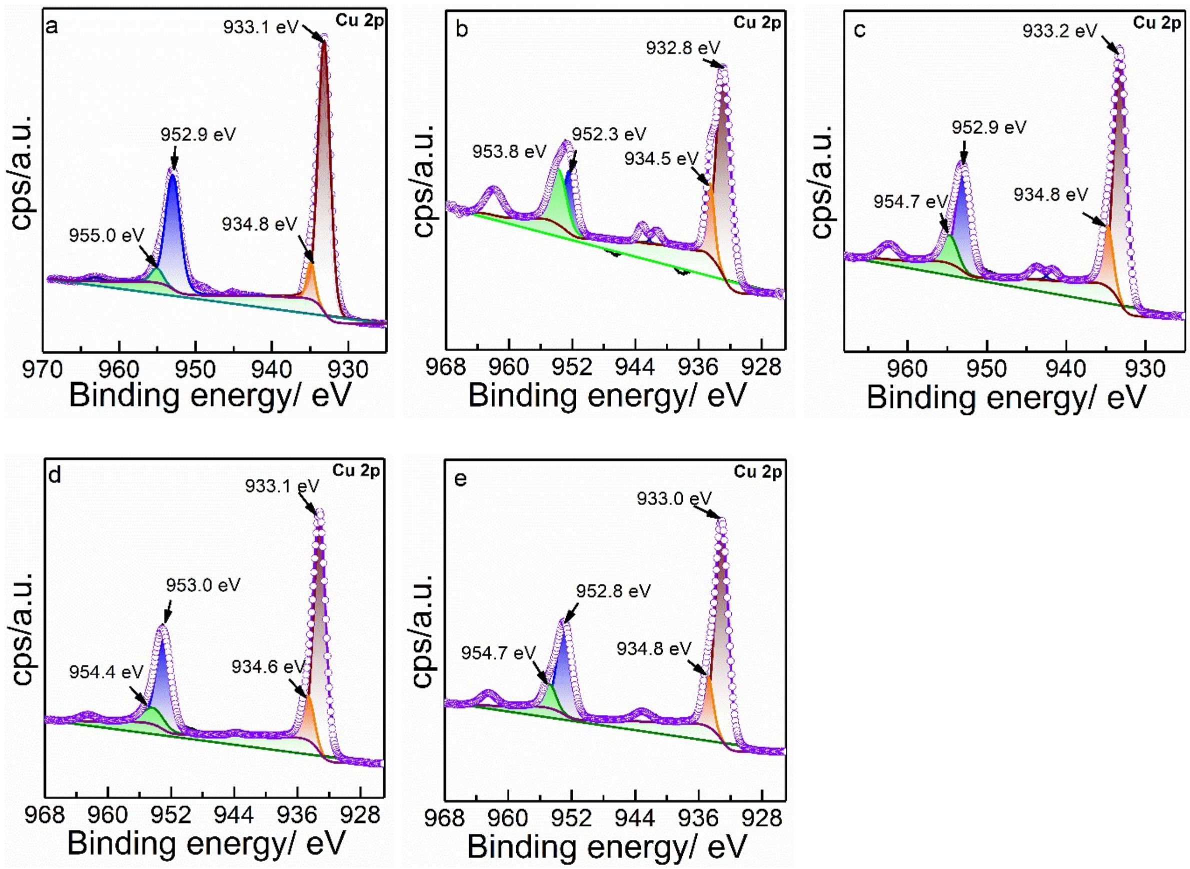

Fig. S9. XPS high resolution Cu 2p spectra of a. pristine Cu-Im MOF, b. Pb adsorbed Cu-Im, c. Mn adsorbed Cu-Im, d. Cd adsorbed Cu-Im and e. Ni adsorbed Cu-Im.

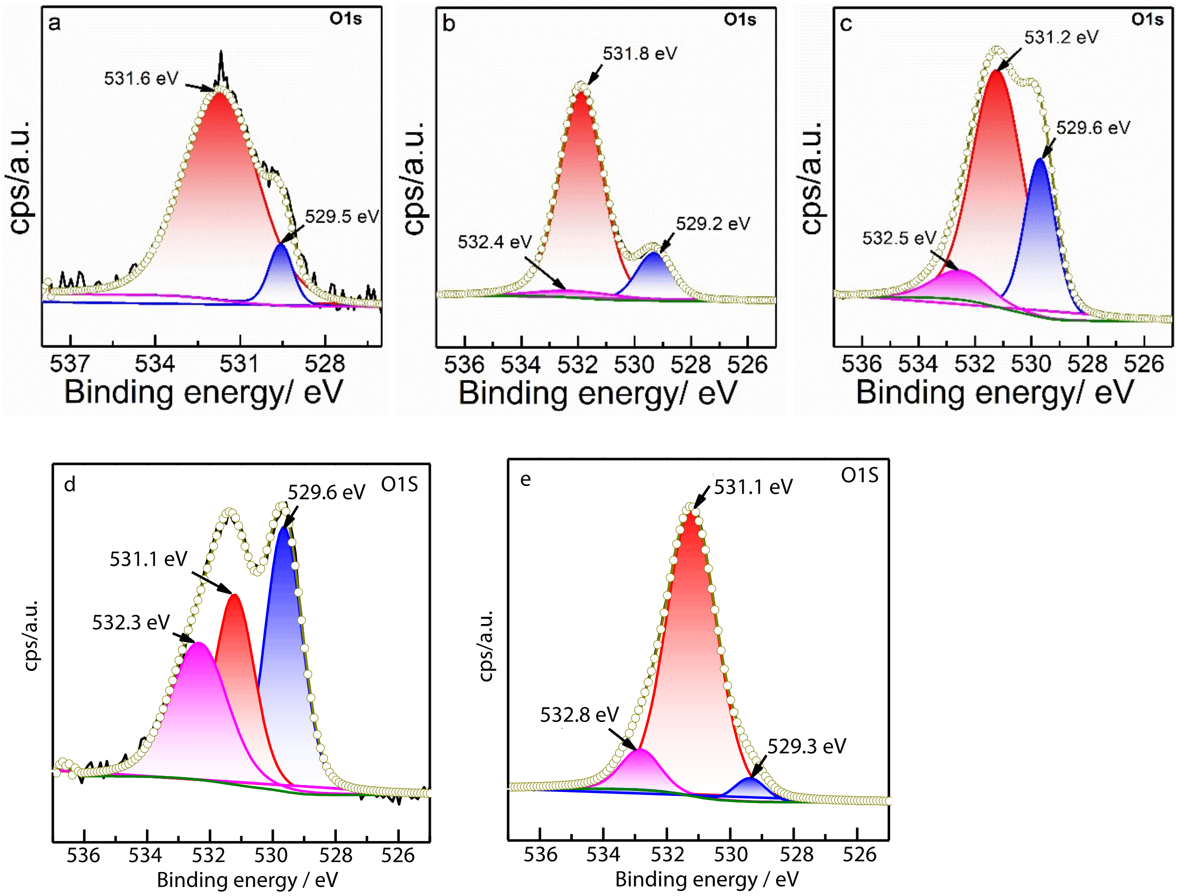

Fig. S10. XPS high resolution O1s spectra of a. pristine Cu-Im MOF, b. Pb adsorbed Cu-Im, c. Mn adsorbed Cu-Im, d. Cd adsorbed Cu-Im and e. Ni adsorbed Cu-Im.

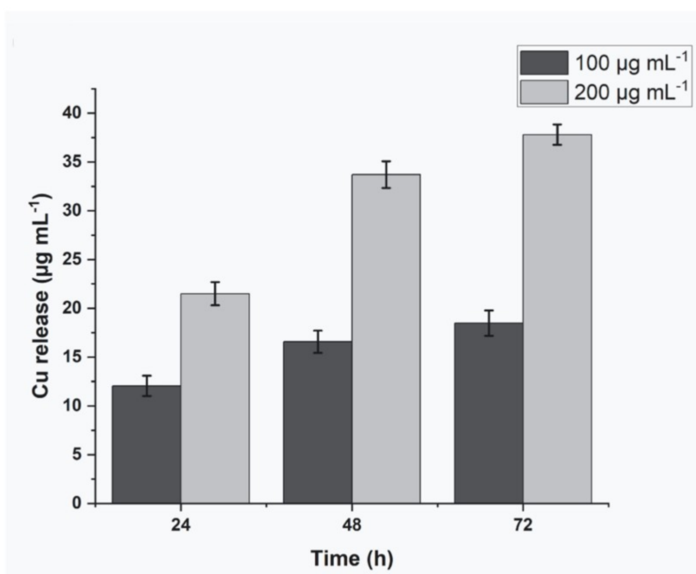

Fig. S11. Cu leaching from Cu-Im framework as a function of time at concentrations of 100 μg mL^{-1} and 200 μg mL^{-1}.

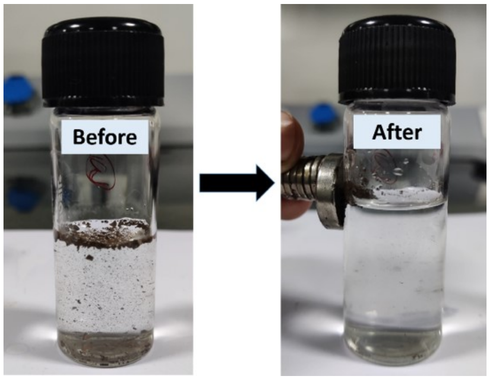

Fig. S12 Images of MOF-magnetic nanoparticle hybrids which could be used to effectively separate the MOF particles from water

Table S1. List of various MOF-based and other adsorbents used for Pb(II), Cd(II) capture from water, as depicted in Figure 6c in the manuscript.

	Material Name	Pb (II) Adsorption Capacity (mg g^{-1})	Cd (II) Adsorption Capacity (mg g^{-1})	Mn(II) Adsorption Capacity (mg g^{-1})	Ni(II) Adsorption Capacity (mg g^{-1})	Ref
1.	Cu-Im	490	327	233	72	This work
2.	dithizone-modified Fe_3O_4 nanoparticles and copper-(benzene-1,3,5-tricarboxylate) MOF nanocomposite	108	188		98	Ref[4]
3.	TMU-5	281	43			Ref[5]
4.	MOF-199 containing magnetite (Fe_3O_4) nanoparticles carrying covalently immobilized 4-(thiazolylazo) resorcinol (Fe_3O_4@TAR)	185	210		196	Ref[6]
5.	MOF-808-EDTA	313				Ref[7]
6.	MIL-101(Fe)	198	155			Ref[8]
7.	UiO-66-EDA	243	217			Ref[9]
8.	MOF-based melamine foams	422	222			Ref[10]
9.	UiO-66-SO_3H	176	194			Ref[11]
10.	Zr-MOF (free carboxylic group)	100	37			Ref[12]
11.	HS-mSi@MOF-5	312	98			Ref[13]
12.	Fe3O4-ZrMOF@GSH	409	403			Ref[14]
13.	UiO-66-NHC(S)NHMe	232	49			Ref[15]
14.	Fe3O4@UiO-66–NH2	833	714			Ref[16]
16.	UiO-66 with melamine	175	146			Ref[17]
17.	DNPH modified -Al_2O_3	100	83	6	18	Ref[18]
18.	Hydrated ferric oxide	211	147			Ref[19]
19.	Calcium titanate	124	8			Ref[20]
20.	Plasma modified biochar	123	61			Ref[21]
21.	MCs@Mg/Fe-LDHs	759				Ref[22]
22.	Chitosan/GO nanofibers	461				Ref[23]
23.	Oxidized MWCNTs	75	66		59	Ref[24]
24.	Na-Y/ZnO/NH_2/SH composite	295			177	Ref[25]
25.	ultrafine mesoporous	85	79		66	Ref[26]

	magnetite (Fe_3O_4) nanoparticles (UFMNPs)					
26.	EDTA-GO	508				Ref[27]
27.	Zeolite NaY	454				Ref[28]
28.	Magnetic Nanoparticle/Nanocomposite Beads	23	12			Ref[29]
29	poly (sodium acrylate)-graphene oxide (PSA-GO)		238	238		Ref[30]
30	ZIF-8/PAN Nanofibers		127			Ref[31]
31	Unmodified Nigerian kaolinite clay (UAK)			111	166	Ref[32]
32	NaCl-activated clinoptilolite+mordenite			21		Ref[33]

Dataset S1 (attached as a CSV file contains the list of MOFs used for the benchmark studies). Under the common name, the attached number corresponds to the reference in Burtch et al.[2] from where the metal centre and linker are extracted. The linker is represented using the SMILES format[3], making it easily featurizable for t-SNE visualisation.

References.

1. J. W. Osterrieth, et al., **2022** How reproducible are surface areas calculated from the BET equation?. *Advanced Materials*, *34*(27) 2201502.
2. N.C Burtch, H. Jasuja, K. S. Walton, **2014** Water stability and adsorption in metal–organic frameworks. *Chemical Reviews*, *114*(20), 10575.
3. D. Weininger, SMILES, a chemical language and information system. 1. **1988** Introduction to methodology and encoding rules. *Journal of Chemical Information and Computer Sciences*, *28*(1), 31.
4. Taghizadeh, M., et al **2013**. A novel magnetic metal organic framework nanocomposite for extraction and preconcentration of heavy metal ions, and its optimization via experimental design methodology. *Microchimica Acta*, *180*, 1073.
5. Tahmasebi, E., et al **2015**. Application of mechanosynthesized azine-decorated zinc (II) metal–organic frameworks for highly efficient removal and extraction of some heavy-metal ions from aqueous samples: a comparative study. *Inorganic chemistry*, *54*(2), pp.425-433.
6. Ghorbani-Kalhor, E., **2016**. A metal-organic framework nanocomposite made from functionalized magnetite nanoparticles and HKUST-1 (MOF-199) for preconcentration of Cd (II), Pb (II), and Ni (II). *Microchimica Acta*, *183*, 2639.
7. Peng, Y., et al **2018**. A versatile MOF-based trap for heavy metal ion capture and dispersion. *Nature communications*, *9*(1), 187.
8. Babazadeh, M., et al **2015**. Solid phase extraction of heavy metal ions from agricultural samples with the aid of a novel functionalized magnetic metal–organic framework. *RSC Adv.*, *5*(26), 19884.
9. Ahmadijokani, F., et al **2021**. Ethylenediamine-functionalized Zr-based MOF for efficient removal of heavy metal ions from water. *Chemosphere*, *264*, 128466.
10. Hu, Q., et al**. 2021**. Ultrastable MOF-based foams for versatile applications. *Nano Res.*, pp.1-10.
11. Gul, S., et al. **2022**. Effective adsorption of cadmium and lead using SO3H-functionalized Zr-MOFs in aqueous medium. *Chemosphere*, *307*, p.135633.
12. Nimbalkar, M.N. and Bhat, B.R., **2021**. Simultaneous adsorption of methylene blue and heavy metals from water using Zr-MOF having free carboxylic group. *Journal of Environmental Chemical Engineering*, *9*(5), 106216.
13. Zhang, J., et al. **2016**. Exploring a thiol-functionalized MOF for elimination of lead and cadmium from aqueous solution. *Journal of Molecular Liquids*, *221*, 43.

14. Ragheb, E., et al. **2022**. Modified magnetic-metal organic framework as a green and efficient adsorbent for removal of heavy metals. *J. Env. Chem. Eng.*, *10*(2), 107297.
15. Saleem, H., et al. **2016**. Investigations on post-synthetically modified UiO-66-NH2 for the adsorptive removal of heavy metal ions from aqueous solution. *Microporous and Mesoporous Materials*, *221*, 238.
16. Abdel-Magied, A.F., et al. **2022**. Magnetic metal-organic frameworks for efficient removal of cadmium (II), and lead (II) from aqueous solution. *J. Env. Chem. Eng.*, *10*(3), 107467.
17. Abdelmoaty, A.S., et al. **2022**. High performance of UiO-66 metal–organic framework modified with melamine for uptaking of lead and cadmium from aqueous solutions. *Journal of Inorganic and Organometallic Polymers and Materials*, *32*(7), 2557.
18. Afkhami, A., et al. **2010**. Simultaneous removal of heavy-metal ions in wastewater samples using nano-alumina modified with 2, 4-dinitrophenylhydrazine. *J. Haz. Mat.*, *181*(1-3), 836.
19. Manju, G.N., et al. **2002**. An investigation into the sorption of heavy metals from wastewaters by polyacrylamide-grafted iron (III) oxide. *Journal of Hazardous materials*, *91*(1-3), 221.
20. Zhang, D., **2011**. Preparation and characterization of nanometer calcium titanate immobilized on aluminum oxide and its adsorption capacity for heavy metal ions in water. *Advanced Materials Research*, *152*, 670.
21. Liu, C. and Zhang, H.X., **2022**. Modified-biochar adsorbents (MBAs) for heavy-metal ions adsorption: A critical review. *Journal of Environmental Chemical Engineering*, *10*(2), 107393.
22. Xie, Y., et al. **2019**. Adsorption behavior and mechanism of Mg/Fe layered double hydroxide with Fe3O4-carbon spheres on the removal of Pb (II) and Cu (II). *Journal of colloid and interface science*, *536*, 440.
23. Najafabadi, H.H., et al. **2015**. Removal of Cu 2+, Pb 2+ and Cr 6+ from aqueous solutions using a chitosan/graphene oxide composite nanofibrous adsorbent. *Rsc Advances*, *5*(21), 16532.
24. Lasheen, M.R., et al. **2015**. Removal of heavy metals from aqueous solution by multiwalled carbon nanotubes: equilibrium, isotherms, and kinetics. *Desalination and Water Treatment*, *53*(13), 3521.
25. Shoja, F. and Amani, M.A., **2020**. Multi-modification of Na-Y zeolite with ZnO nanoparticles, amine, and mercapto functional groups for single and simultaneous heavy metal adsorption from water system. *Research on Chemical Intermediates*, *46*, 3569.
26. Fato, T.P., et al. **2019**. Simultaneous removal of multiple heavy metal ions from river water using ultrafine mesoporous magnetite nanoparticles. *ACS omega*, *4*(4),7543.
27. Cui, L., et al. **2015**. EDTA functionalized magnetic graphene oxide for removal of Pb (II), Hg (II) and Cu (II) in water treatment: adsorption mechanism and separation property. *Chem. Eng. J.*, *281*,1.
28. Shariatinia, Z. and Bagherpour, A., **2018**. Synthesis of zeolite NaY and its nanocomposites with chitosan as adsorbents for lead (II) removal from aqueous solution. *Powder Technology*, *338*, 744.
29. ŞAHİN, M., et al. **2023**. Removal of Ni (II), Cu (II), Pb (II), and Cd (II) from Aqueous Phases by Silver Nanoparticles and Magnetic Nanoparticles/Nanocomposites. *ACS omega*, *8*(38), 34834.
30. Xu, R., et al. **2015**. New double network hydrogel adsorbent: Highly efficient removal of Cd (II) and Mn (II) ions in aqueous solution. *Chemical Engineering Journal*, *275*, 179.
31. Peng, L., et al. **2020**. Heavy metal elimination based on metal organic framework highly loaded on flexible nanofibers. *Environmental Research*, *188*, 109742.
32. Dawodu, F.A. and Akpomie, K.G., **2014**. Simultaneous adsorption of Ni (II) and Mn (II) ions from aqueous solution unto a Nigerian kaolinite clay. *J. Materials research and technology*, *3*(2), pp.129-141.
33. Taffarel, S.R. and Rubio, J., **2009**. On the removal of Mn2+ ions by adsorption onto natural and activated Chilean zeolites. *Minerals Engineering*, *22*(4), 336.